

Catastrophic Shifts in Semiarid Vegetation-Soil Systems May Unfold Rapidly or Slowly

Derek Karssenberg,^{1,*} Marc F. P. Bierkens,¹ and Max Rietkerk²

1. Department of Physical Geography, Faculty of Geosciences, Utrecht University, PO Box 80115, 3508 TC Utrecht; 2. Copernicus Institute of Sustainable Development, Environmental Sciences Group, Utrecht University, PO Box 80115, 3508 TC Utrecht

Submitted January 5, 2017; Accepted June 5, 2017; Electronically published October 4, 2017

Online enhancements: appendices.

ABSTRACT: Under gradual change of a driver, complex systems may switch between contrasting stable states. For many ecosystems it is unknown how rapidly such a critical transition unfolds. Here we explore the rate of change during the degradation of a semiarid ecosystem with a model coupling the vegetation and geomorphological system. Two stable states—vegetated and bare—are identified, and it is shown that the change between these states is a critical transition. Surprisingly, the critical transition between the vegetated and bare state can unfold either rapidly over a few years or gradually over decennia up to millennia, depending on parameter values. An important condition for the phenomenon is the linkage between slow and fast ecosystems components. Our results show that, next to climate change and disturbance rates, the geological and geomorphological setting of a semiarid ecosystem is crucial in predicting its fate.

Keywords: critical transition, geomorphology, slow transient, model emulation, process-based model, minimal model.

Introduction

A gradual change in a driver of a complex system may result in a critical transition, which is a switch between contrasting equilibrium states (cf. reviews in Beisner et al. 2003; Scheffer 2009). Critical transitions are mostly studied by considering the system in equilibrium with its drivers (e.g., Janssen et al. 2008). The transition then occurs at the tipping point, which is the threshold value of the driver that, once exceeded, results in a considerable change of the system. For studies considering the response of an

ecosystem to changes in drivers over time, this equilibrium assumption implies instantaneous change in the system state when the tipping point has been reached. Recently, however, it has become increasingly clear that ecosystems may exhibit a slow transition between equilibrium states because of a low rate of change in the system when it is pushed over a tipping point (Van Geest et al. 2007; Hughes et al. 2013). As a result, ecosystems may show a delayed response to changes in drivers. Contrary to conventional knowledge, this implies that a critical transition in the system equations may result in a gradual (instead of instantaneous or relatively rapid) change in ecosystem state. This may have important implications for explaining transitions in coupled climate-vegetation-soil systems (Kröpelin et al. 2008; Dusat et al. 2011) and for understanding desertification and land degradation in semiarid regions (Pickup 1999; Thornes 2007; Vicente-Serrano et al. 2012). Also, because slow transitions delay the switch between stable states, they are a determinant of the window of opportunity to repair a collapsed ecosystem (Biggs et al. 2009; Balke et al. 2014). Given these important implications, it is somewhat surprising that slow transitions have thus far received limited attention in ecological research. As a consequence of this limited attention, it remains thus far unknown whether their effect is widespread in ecosystems and whether they consistently appear in a particular ecosystem or sometimes also rapid transitions occur in the same ecosystem.

Here we hypothesize that both slow and rapid transients may appear in an ecosystem, in particular, when the ecosystem contains slow and fast, interacting subsystems, which is the case in many systems, for instance, dune vegetation (Siteur et al. 2016), food webs (Stenseth et al. 1997), evolutionary dynamics (Marrow et al. 1996), and lakes (Van Geest et al. 2007). We take a semiarid ecosystem as an example. In this ecosystem, vegetation growth is interrelated with soil status, and critical transitions are expected to exist that include combined changes in the vegetation and soil compartments of the ecosystem. Veg-

* Corresponding author; e-mail: d.karssenberg@uu.nl.

ORCID: Karssenberg, <http://orcid.org/0000-0002-6475-363X>; Bierkens <http://orcid.org/0000-0002-7411-6562>.

Am. Nat. 2017. Vol. 190, pp. E145–E155. © 2017 by The University of Chicago. 0003-0147/2017/19006-57479\$15.00. All rights reserved. This work is licensed under a Creative Commons Attribution-NonCommercial 4.0 International License (CC BY-NC 4.0), which permits non-commercial reuse of the work with attribution. For commercial use, contact journalpermissions@press.uchicago.edu. DOI: 10.1086/694413

etation responds generally rather quickly to changes in drivers, mostly over months or years, and it is thus hypothesized that it may cause rapid transients of the system as a whole. However, processes changing soil attributes—such as soil formation from bedrock or water erosion—are generally slow, resulting in changes in soil attributes over large periods of time ($\sim 10^1$ – 10^4 years; Schaetzl and Anderson 2005). Because soil properties may affect vegetation growth (Rietkerk and Van De Koppel 1997; Rietkerk et al. 1997; Scheffer et al. 2005; Thornes 2007), changes in the slow soil system might result in a slow transition of the ecosystem as a whole. However, it is unclear how the link between soil and vegetation affects the transient and under what conditions a slow transition might occur. Thus, our key questions are whether both rapid and slow transients occur in semiarid ecosystems and, if this is the case, what mechanisms determine the duration of the transient.

Addressing these questions requires investigating a fully coupled system linking vegetation, water, and soil compartments. Here, we follow this approach by numerical modeling of a semiarid ecosystem. We build on existing studies coupling vegetation and soil evolution (in particular, Thornes 1985, 2007; revisited in Wainwright and Parsons 2010) by including the effect of changes in runoff pattern and soil depth, affecting runoff and water available for the vegetation, and overland flow affecting vegetation growth.

Using a minimal lumped (nonspatial) model of vegetation-soil dynamics, we first investigate the occurrence of a critical transition, which is hypothesized to explain the widely occurring land degradation process (Rietkerk et al. 1997; Thornes 2007) because of overgrazing or climate change. Our study involves a change from a healthy ecosystem with high biomass and thick soils to a system with ultimately zero biomass and bare bedrock. Next, we investigate how rapidly the critical transition unfolds and how the speed of the transient depends on the value of key ecosystem parameters. We use simulations with a more complex spatially explicit model to support the identification of the minimal model and to evaluate whether it shows the same qualitative behavior as the minimal model.

The Minimal Model

Critical transitions in modeled systems are mostly studied using minimal models (*sensu* Van Nes and Scheffer 2005), because these lumped analytical models enable finding system properties—in particular, fixed points (stable equilibria)—through analytical analysis. Here we follow the same approach. In the identification of the minimal model equations, however, we cannot fully rely on existing studies because current studies that use minimal models often do not include soil evolution and erosion, apart from

Thornes (1985, 2007; revisited in Wainwright and Parsons 2010). Therefore, we use simulations of a spatially explicit model—with a conceptualization of processes that are mostly validated in the literature—to support the identification of the equations and parameters of the minimal model. In addition, the spatially explicit model is used to evaluate whether it shows the same qualitative behavior as the minimal model. By following this approach, we believe that the strengths of minimal models (allowing analytical analysis) and spatially explicit models (capturing processes in more detail) are combined, increasing the credibility of the models.

Before introducing the minimal model, we first provide key references to process descriptions of the spatially explicit model on which it is based (details provided in app. A; apps. A–F are available online). The hydrological component of the model represents rainfall, evapotranspiration, rainfall canopy interception, infiltration, and overland flow (Rodríguez-Iturbe and Porporato 2004; Karssenberg 2006; Broksma et al. 2010). Vegetation is simulated by biomass growth, biomass maintenance, and diffusion equations (Noy-Meir 1975; Rodríguez-Iturbe and Porporato 2004). Changes in soil thickness over time are governed by soil formation through bedrock weathering, soil creep, and erosion of soil material (Morgan and Duzant 2008; Heimsath and Burke 2013). Multiple couplings between hydrology, vegetation, and soil have been incorporated. The model represents an 80×40 -m hillslope.

The equations of the minimal model are derived from the spatially explicit model by incorporating its process equations in a lumped fashion or using simplified conceptual representations of spatial processes. As a result, a parameter in the minimal model often lumps multiple, spatial, processes. It is therefore hard to identify realistic lumped parameter values from literature or expert opinion. To circumvent this problem, the spatially explicit model was run with inputs typical for semiarid ecosystems, and the parameters of the minimal model were then tuned to the output of the spatially explicit model. This set of parameter values of the minimal model can be considered representative of a semiarid ecosystem referred to below as the standard ecosystem. Appendix B gives a more extensive description of the methodology used to identify the minimal model and its parameters.

The minimal model consists of two differential equations. The parameter values given below are those of the standard ecosystem. The change in biomass B (kg m^{-2}) is modeled as

$$\frac{dB}{dt} = \begin{cases} [1 - (1 - i)e^{-D/d}] \left[rB \left(1 - \frac{B}{c} \right) \right] - g \left(\frac{B}{s + B} \right) & \text{for } B \geq 0 \\ 0 & \text{for } B = 0 \end{cases} \quad (1)$$

(fig. 1E). The first term is the growth rate dependence on soil depth and biomass (fig. 1A). The second part of the first term corresponds to the well-known overharvesting model (Noy-Meir 1975; May 1977), which was shown to be applicable to vegetation growth in semiarid regions (cf. Thornes 2013), with growth rate r (2.1 years^{-1}) and carrying capacity c (2.9 kg m^{-2}) representing the growth rate for an infinite thick soil. The growth rate reduces with decreasing soil depth because a larger proportion of net rain is lost to overland flow as a result of increased saturated overland flow. In addition, because of increased overland flow, damage to the vegetation increases as a result of seed loss (Yu et al. 2016) and rill and gully formation (Valentin et al. 2005). This is represented by the first part of the first term, which is between i and 1, where i (-0.7) is the reduction factor at zero soil depth and d (0.04 m) is a soil depth range parameter. The second term (fig. 1C) represents graz-

ing, modeled with the Michaelis equation, which is supported by experimental data (cf. Noy-Meir 1975). It uses g , the grazing pressure (which is $1.76 \text{ kg m}^{-2} \text{ year}^{-1}$ in fig. 1), and s (0.4 kg m^{-2}), the biomass where the grazing is $0.5g$.

The change in the soil depth D (m) is

$$\frac{dD}{dt} = \begin{cases} W_0 e^{-aD} - e^{-B/b} [E_i + e^{-D/k} (E_0 - E_i)] - C & \text{for } D \geq 0 \\ 0 & \text{for } D = 0 \end{cases} \quad (2)$$

(fig. 1F). The first term represents soil formation, which is bedrock recession normal to the surface by bedrock weathering (fig. 1B) and is the same as the exponential function used in the spatial model. The exponential form is well constrained by a number of empirical studies (Heimsath and Burke 2013; Larsen et al. 2014; Stockmann et al. 2014). It uses the soil formation rate W_0 ($5 \times 10^{-4} \text{ m year}^{-1}$) for

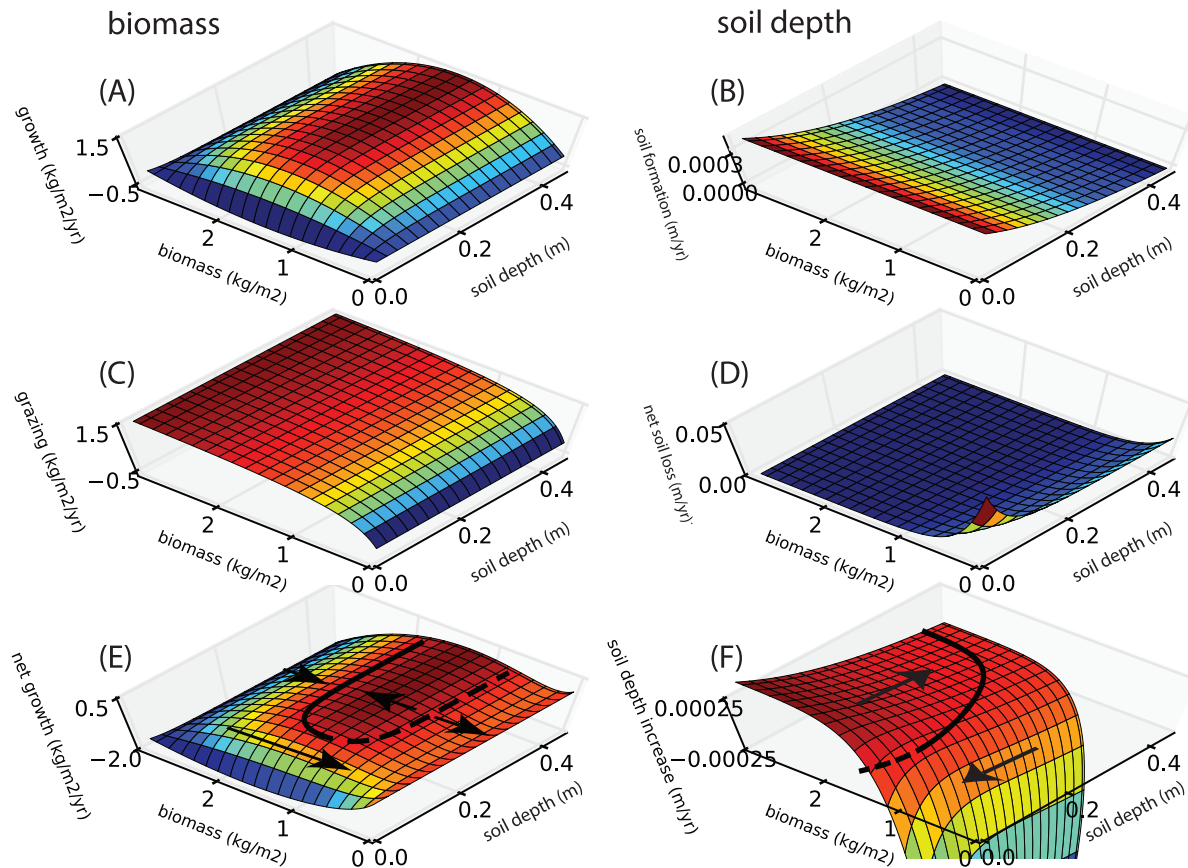


Figure 1: Terms of minimal model equations (1) and (2) plotted against biomass B and soil depth D for default parameter values of the standard ecosystem, resulting in a stable equilibrium. Vegetation system: vegetation growth term (A), grazing term (C), and net growth dB/dt (i.e., growth term minus grazing term; E). Soil system: soil formation (B), soil loss (water erosion plus creep terms; D), and net soil depth increase dD/dt (i.e., soil formation minus soil loss; F). Solid line, stable nullcline; dashed line, unstable nullcline. Arrows indicate direction of change.

bedrock without a soil cover ($D = 0$) and the soil formation exponent a (4.0 m^{-1}). The second term and the third term represent soil loss (fig. 1D). The second term is soil loss due to water erosion. It uses E_r , which should be interpreted as the erosion rate ($0.021 \text{ m year}^{-1}$) at zero biomass and an infinite soil depth. When soil depth reduces, the erosion increases because of the reduced maximum water storage of the soil, resulting in an increased overland flow generated by saturation of the soil. This effect is represented by E_0 , which is the erosion rate ($0.084 \text{ m year}^{-1}$) reached when soil depth approaches 0 (note that at zero soil depth, no erosion will occur), and the parameter k (0.05 m^{-1}), determining the dependence of erosion on soil depth. When biomass B increases, erosion decreases mainly because of increased rainfall interception and increased infiltration capacity of the soil, reducing runoff. This is represented by the exponent containing b ($0.28 \text{ m}^2 \text{ kg}^{-1}$), using an exponential form corresponding to findings from empirical studies (cf. Thornes 2013). The third term, C ($1 \times 10^{-4} \text{ m year}^{-1}$) is the soil loss by creep, which is taken equal to the fall of the drainage level at the bottom of the hillslope. By setting the rates of change given by equations (1) and (2) to 0, the two equations of equilibria for the vegetation and soil subsystems are found, referred to here as nullclines. Appendix E gives these equations and a number of other mathematical properties of the minimal model.

Properties of the Minimal Model

The minimal model represents key processes of the vegetation-soil system. The vegetation system is determined by biomass growth (fig. 1A) and grazing terms (fig. 1C). The biomass growth term decreases in magnitude with decreasing soil thickness. At a high soil thickness, biomass growth is positive and the growth term in equation (1) reduces to the growth equation used by Noy-Meir (1975). Below a soil thickness of $\sim 0.15 \text{ m}$, biomass growth reduces considerably, even becoming negative at very low soil thickness values (fig. 1A). This is due to an increased loss of rainfall water to overland flow when the soil depth becomes smaller, resulting in a smaller amount of water available for the vegetation. Also, the increased overland flow causes an increase in direct damage to the vegetation during rainfall events, which is why the biomass growth term becomes negative at low values of the soil thickness. The reduction in the value of the biomass growth with reducing soil depth has a profound effect on the behavior of the vegetation subsystem. A tipping point occurs in the vegetation subsystem at a soil depth value of $\sim 0.1 \text{ m}$. Above this value, the soil is sufficiently thick to support a vegetation cover and a stable equilibrium exists (fig. 1E), in addition to an unstable one. Below this soil depth, biomass collapses to zero biomass.

Soil depth is determined by soil formation and soil loss. The soil formation increases with decreasing soil depth (fig. 1B) in the same manner for all values of biomass, because it is assumed that the amount of biomass has a negligible effect on soil formation. The soil loss increases considerably with decreasing biomass (fig. 1D), in particular, below biomass values of approximately 1 kg m^{-2} . This is caused by an increase in net rain reaching the soil, resulting in increased erosion by raindrop impact and overland flow. In a similar fashion, soil loss increases with decreasing soil depth, particularly below a soil thickness of $\sim 0.15 \text{ m}$, which is due to the reduced water storage capacity of thinner soils, resulting in an increased overland flow due to saturated soil conditions. However, this increase is negligible at higher biomass values (fig. 1D), because higher biomass results in increased evapotranspiration (which keeps the soil dry) and increased rainfall interception, resulting in a less saturated overland flow. A change in the behavior of the soil system occurs at a vegetation cover of $\sim 1.3 \text{ kg m}^{-2}$ (fig. 1F). Above this value, the biomass is sufficiently high to protect the soil, and the direction of change in the soil system (when keeping vegetation cover fixed) is toward the stable nullcline of the soil system, as indicated by the arrow in figure 1F. Below this value, the direction of change in the soil system is toward zero soil depth (when vegetation cover is fixed), as indicated by the second arrow in figure 1F.

When both subsystems are in stable equilibrium, the ecosystem is in equilibrium, which is represented by the intersection of the nullclines, as shown by the red circle in figure 2A. A small disturbance of the system pushing it away from this equilibrium would lead to a return to its equilibrium, along the lines shown in figure 2B. Larger disturbances resulting in a change in system state below either roughly 0.1 m soil depth or 0.6 kg m^{-2} biomass would lead to collapse of the system, as indicated by the arrows in figure 2A directed toward the origin; that is, $D = B = 0.0$. A second intersection between the nullclines appears in figure 2A at a lower biomass and soil depth. Appendix E describes all properties of the model, including bifurcation diagrams.

The system considered here contains slow and fast subsystems. The soil subsystem shows low rates of change. For most combinations of soil depth and biomass, the rate of change in soil depth is $2 \times 10^{-4} \text{ m year}^{-1}$ (fig. 1F), which is equal to a change in soil depth per year of about 0.05% of the soil depth. At lower values of biomass and soil depth, the magnitude of change increases (fig. 1E), but even then it will remain below a 20% change in soil depth per year. The vegetation system is faster responding, and rates of change are often up to 25%–100% per year. Thus, our system can be considered a slow-fast system, although there is not a complete separation of timescales that would

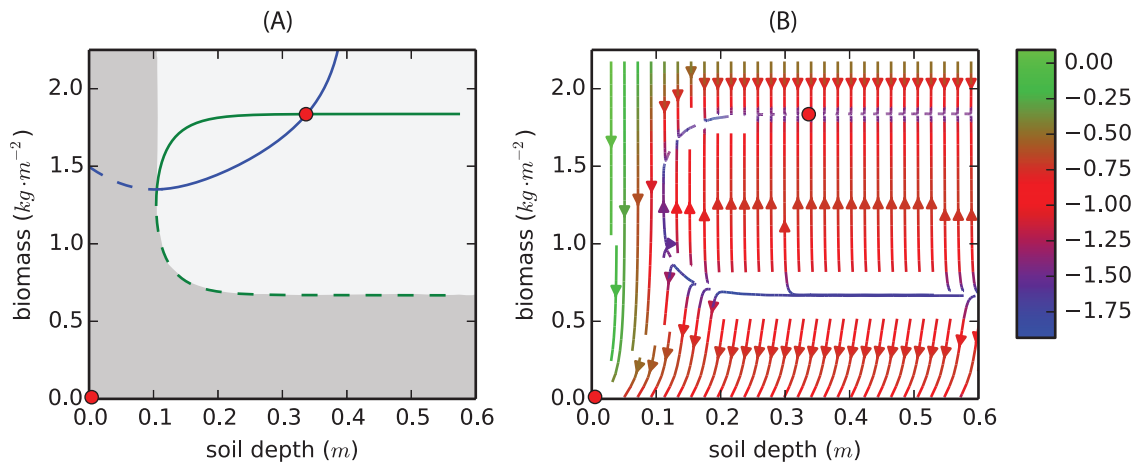


Figure 2: Properties of the minimal model, default parameters of the standard ecosystem values resulting in a stable equilibrium. A, Stable (solid line) and unstable (dashed line) nullcline of soil subsystem (blue line) and vegetation subsystem (green line). Gray shading indicates basins of attraction. B, Direction and rate of change. Color scale represents log transformed values. Red circles, stable system equilibria (fixed point).

allow application of the singular perturbation approach described by Rinaldi and Scheffer (2000) and Solé (2011).

Duration of Transients between Stable Equilibria

A change in a driver (i.e., external forcing) of the system may lead to a shift of the ecosystem and a transient toward zero biomass and soil depth. It is somewhat arbitrary which of the parameters in our model is chosen as driver, because many parameters may be influenced by ecosystem management or climate. Here we take grazing pressure g as the driver. The remaining parameters are considered ecosystem properties.

Let us see then how changes in grazing pressure may lead to a critical shift. When the grazing pressure is increased, the nullcline for the vegetation subsystem shifts to lower biomass values and lower soil depth values. As a result, the fixed point (red circle in fig. 2A) moves along the stable equilibrium part of the nullcline of the soil subsystem, which does not change position when grazing pressure is changed, in the direction of lower biomass and soil depth values. When grazing pressure continues to increase, this ultimately leads to the situation where the stable nullclines of the two subsystems become separated and do not intersect anymore. The disappearance of the intersection between the nullclines corresponds to the critical transition. This situation with a grazing pressure just above the critical transition is evaluated for two ecosystems, one with a carrying capacity $c = 2.3 \text{ kg m}^{-2}$ and one with $c = 3.5 \text{ kg m}^{-2}$ (fig. 3A, 3B), referred to as the low and high carrying capacity ecosystems, respectively. All other parameters have a value of the standard

ecosystem. The critical transition is reached at a grazing pressure of $g = 1.4 \text{ kg m}^{-2} \text{ year}^{-1}$ and $g = 2.3 \text{ kg m}^{-2} \text{ year}^{-1}$ for the low and high carrying capacity ecosystems, respectively.

We analyze the transients from the system state at the critical transition to the complete collapse of the system using these two ecosystems. The low carrying capacity ecosystem has a transient consisting of three phases (fig. 3A). In the first phase, soil depth decreases slowly because of low rates of change in soil depth at this state of the system. The change follows the nullcline of the vegetation system, and thus biomass also decreases, but slowly. In the second phase, the vegetation subsystem collapses much more rapidly because of high rates of change in vegetation biomass. Finally, when vegetation has disappeared, soil depth decreases rapidly because of high net erosion rates at zero biomass (visible in fig. 3E and clearly visible by the large negative values of soil depth increase in fig. 1F at low biomass values). Surprisingly, the first phase has a very short duration in the high carrying capacity ecosystem (fig. 3B); the critical transition unfolds by a direct, rapid collapse of the vegetation subsystem. Because of these differences, the low carrying capacity ecosystem collapses in about 2,000 years, while for the high carrying capacity ecosystem this takes only about 25 years (fig. 4A).

A comparable effect is found when comparing two ecosystems that differ regarding the soil subsystem. Figure 3C and 3D shows results for two ecosystems that differ in bare bedrock soil formation rate W_0 and the parameter a . These parameters are chosen such that both scenarios have an equilibrium soil thickness of 0.4 m at high biomass values (representing a situation without wash erosion; i.e., soil

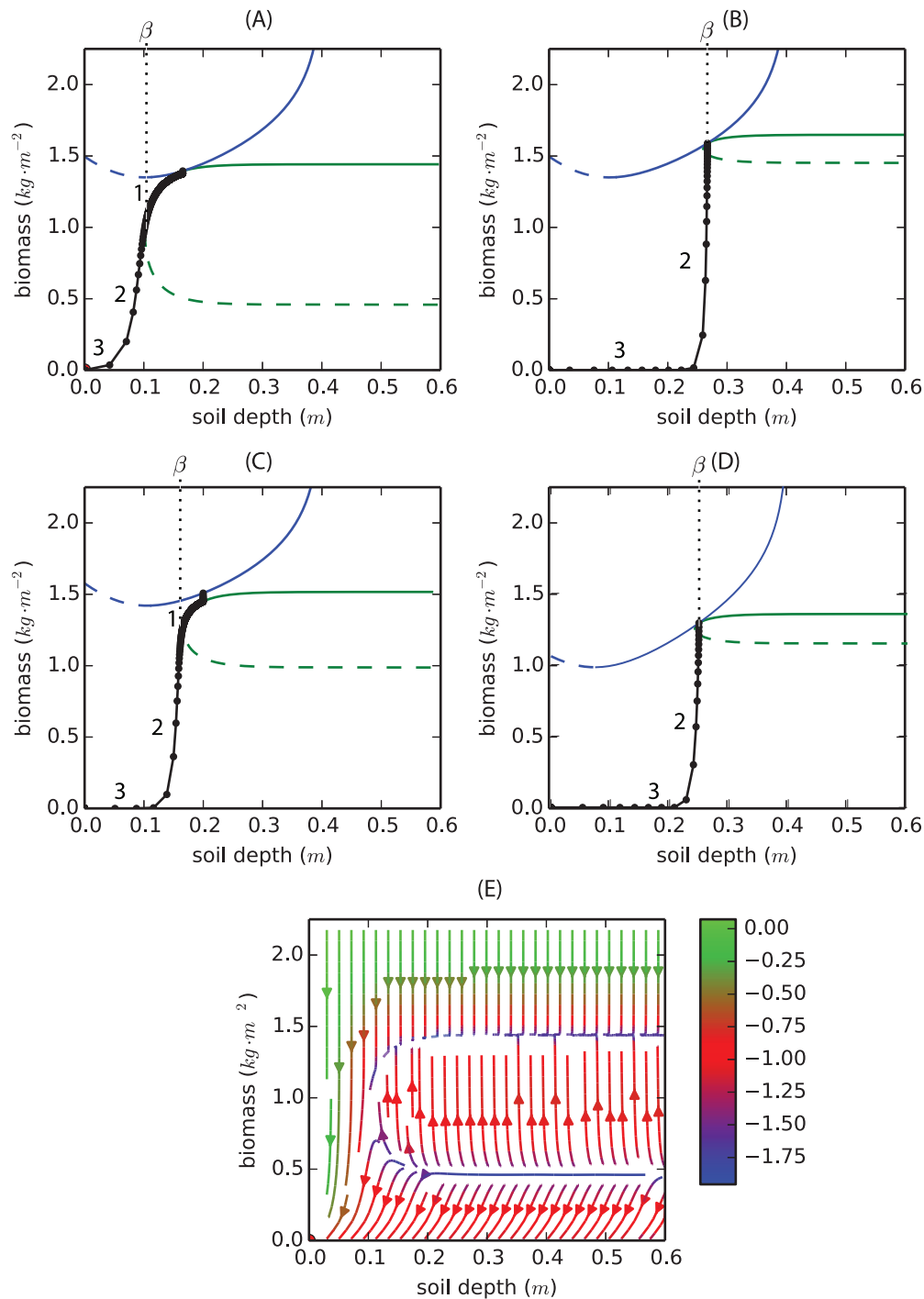


Figure 3: Stability, transients, and rate of change of the minimal model, with grazing pressure just above the value at the catastrophic shift. A, Low carrying capacity ecosystem ($c = 2.3 \text{ kg m}^{-2}, g = 1.4 \text{ kg m}^{-2} \text{ year}^{-1}$). B, High carrying capacity ecosystem ($c = 3.5 \text{ kg m}^{-2}, g = 2.3 \text{ kg m}^{-2} \text{ year}^{-1}$). C, Low bare bedrock soil formation ecosystem ($W_0 = 0.0004 \text{ m year}^{-1}, a = 3.47, g = 1.90 \text{ kg m}^{-2} \text{ year}^{-1}$). D, High bare bedrock soil formation ecosystem ($W_0 = 0.002 \text{ m year}^{-1}, a = 7.49, g = 1.96 \text{ kg m}^{-2} \text{ year}^{-1}$). The remaining parameters are those of the standard ecosystem. Nullclines are given by blue (soil system) and green (vegetation system) lines (solid lines, stable equilibrium; dashed lines, unstable equilibrium). Black lines indicate transient simulations, and each circle represents 1 year; 1–3 indicate phases during the transient. β , minimum soil depth with stable vegetation subsystem (m). E, Low carrying capacity ecosystem, direction, and rate of change; color scale represents log transformed values.

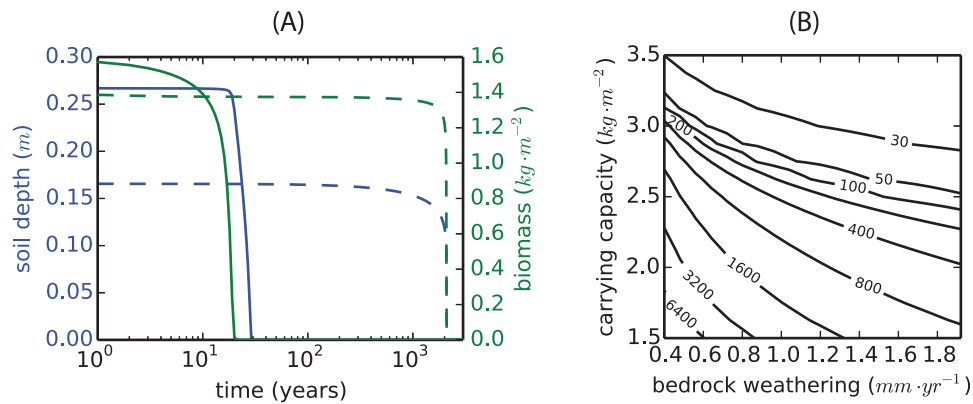


Figure 4: A, Transients for high (solid lines) and low (dashed lines) carrying capacity ecosystems (blue, soil depth; green, biomass); log scale on X-axis. B, Duration of transient (i.e., duration from critical shift to complete collapse; years) as a function of bare bedrock weathering (i.e., soil formation for bare bedrock) and carrying capacity, calculated from the minimal model.

formation equals creep rates), using W_0 and a values comparable to those observed in the field (Heimsath and Burke 2013; Larsen et al. 2014; Stockmann et al. 2014). In the low bare bedrock weathering ecosystem (fig. 3C), the ecosystem stays for a long duration in phase 1, resulting in long duration of the transient. In the high bare bedrock weathering ecosystem (fig. 3D), phase 1 does not occur, and the transient occurs almost instantaneously.

Figure 4B shows the duration of the transient for all combinations of values for carrying capacity and bedrock weathering, indicating a comparable sensitivity to both parameters. In fact, the duration of the transient is sensitive to almost all minimal model parameters, as shown by sensitivity analyses (app. C).

Discussion

The most important result of our study is that the critical transition may unfold rapidly or slowly and that changing only a single ecosystem parameter may cause the ecosystem to have a rapid or slow transient. This holds for a large number of ecosystem parameters.

Essential to the occurrence of this phenomenon of either slow or rapid transients is the existence of two interconnected subsystems, with very different rates of change when pushed over the critical point. The duration of the transient then depends on whether the shift occurs first along the slow or first along the fast subsystem. For our modeled ecosystems with a slow shift (fig. 3A, 3C), the vegetation system still has a stable nullcline that extends from the critical point toward lower soil depth and biomass values. At the start of the transient, the system follows this nullcline; that is, the vegetation system remains in equilibrium while the soil system is collapsing, which occurs

very slowly because of the limited capability of the soil system to adjust its state. Only after a long time, the vegetation system is pushed over its critical point, and the whole system collapses in a short period of time. This slow transient corresponds to an ecosystem where the vegetation is able to persist even at soil thickness values below those occurring at the critical point. At a grazing pressure just above the threshold value, vegetation is stable but too limited to sufficiently protect the soil against erosion. Consequently, the removal of soil material becomes somewhat larger than formation of soil material through bedrock weathering, resulting in a slow decrease in soil thickness. After a long time of ongoing decrease in soil thickness, the soil reaches a thickness not sufficient for the vegetation to sustain because soil water storage required for vegetation growth becomes too limited, and at lower soil thicknesses, saturated overland flow during intense rainstorms causes damage to the vegetation. As a result, biomass values quickly decrease. Finally, at very low or zero vegetation cover, the soil depth collapses quickly because of relatively large raindrop impact and overland flow causing large amounts of erosion. For our modeled ecosystems with a rapid shift (fig. 3B, 3D), the opposite happens. Already at soil thickness values just below those of the critical point, the vegetation is not capable of sustaining a healthy state. Consequently, the transient starts with a rapid collapse of the vegetation system, followed by a rapid collapse of the soil system due to removal of the vegetation cover protecting the soil.

Our findings are confirmed by transient model runs with the spatially explicit model of our ecosystem, which also indicate the existence of two fixed points, hysteresis, and the occurrence of slow or fast transitions (app. D). Because the spatially explicit model relies on model components that have been tested in other studies, as described

in appendix A, these results increase credibility of our findings. Improvements to the spatially explicit model, however, are required in future studies. These include verification, calibration, and evaluation (*sensu* Oreskes et al. 1994) of the model, exploring the effect of different process representations (e.g., Pelletier et al. 2013) and inclusion of processes not represented in our model, in particular, the soil-plant nutrient cycle. In addition, our approach would gain by using more sophisticated dynamic model emulation methods (Castelletti et al. 2012).

Our model results give strong indications for the existence of slow (or rapid) transients between stable equilibria in real-world semiarid soil-vegetation systems. However, field studies thus far have not yet provided explicit proof for the existence of this type of slow transients in the ecosystem studied. This is mainly because direct evidence could possibly be provided only by observational data collected in ecosystems with known changes in the magnitude of the drivers over extensive periods of time (i.e., 10^2 – 10^3 years). This type of data is sparse if not non-existent. A possible approach is the use of time series of remote sensing data (de Jong et al. 2011; Vicente-Serrano et al. 2012), which provides data with a large spatial extent but still limited duration of decennia. An alternative approach is reconstruction of ecosystem evolution using paleoecological data (e.g., Duser et al. 2011), providing information for much longer time spans, however, often without exact knowledge of the magnitude and variation in drivers and the ecosystem configuration. Thus, the challenges in finding direct evidence are considerable, and our study confirms the need for long time series of ecological data (Willis et al. 2010; Davies et al. 2014).

It would be valuable for ecosystem management to be able to predict whether a particular ecosystem has slow or fast transients. In the case of a slow transient, for instance, there is ample time to prevent a shift from unfolding completely, because during the transient, the ecosystem state shows relatively little change, and minor changes in an ecosystem driver may still bring the system back to a healthy state. Estimating the duration of the transient in real-world ecosystems beforehand is, however, not an easy task. One approach is to estimate the parameter values in our minimal model from field observations and to use this information to estimate the duration of the transient. For instance, ecosystems with a high carrying capacity will tend to have shorter transients. Another approach is to evaluate the ecosystem state at the brink of collapse, that is, with a grazing pressure just before or over the critical point. Ecosystems with a minimum soil depth with a stable biomass (β in fig. 3A–3D) much smaller than the soil depth at the critical point will have a slow transient, because these will have a pronounced phase 1 in the transients. Ecosystems where the minimum soil depth with a stable biomass

is close to the soil depth observed at the shift will have a fast transient (cf. app. F).

Although direct empirical corroboration of the occurrence of slow transients in arid ecosystems is lacking, our study does provide new insight for current research and management. The possibility of occurrence of slow transients implies that very slow degradation of semiarid ecosystems observed nowadays does not always need to refer to an ecosystem in equilibrium with a slowly changing driver; instead, it can be an indication of a system that is already over its tipping point but in a slow transient state toward a degraded ecosystem. Thus, a slow transient might be an alternative or additional explanation of slow changes in semiarid ecosystems observed (e.g., Vicente-Serrano et al. 2012). Another important implication of our study is that critical transitions in the climate-vegetation-soil system could be delayed by connections between vegetation and geomorphology, and these connections might have contributed to observed slow transitions in climate-vegetation-soil systems in addition to plant diversity, as described by Claussen et al. (2013).

An important question is whether the observed slow-fast divergence of the transient is a universal phenomenon that occurs in many other ecosystems. The lake ecosystem described by Van Geest et al. (2007) has a slow transient caused by a phenomenon similar to the one described here. However, the study does not provide an extensive analysis of whether rapid transients occur and under what ranges of parameter values. As shown in our study, a requirement of a slow-fast divergence of the transient is the existence of interconnected fast and slow subsystems because this enables the divergence of the transient. A very large number of ecosystems exist with coupled slow and fast components, including consumer resource ecosystems (Ludwig et al. 1978; Stenseth et al. 1997), evolutionary ecosystems (Marrow et al. 1996), and coupled geomorphological ecological systems (Werner 1999; Van Geest et al. 2007; Siteur et al. 2016). However, whether these ecosystems indeed show a slow-fast divergence of the transient also depends on how the slow and fast subsystems are connected and on the position and shape of the nullclines along the range of the system parameters.

Acknowledgments

We thank the anonymous reviewers for helpful comments on early versions of the manuscript.

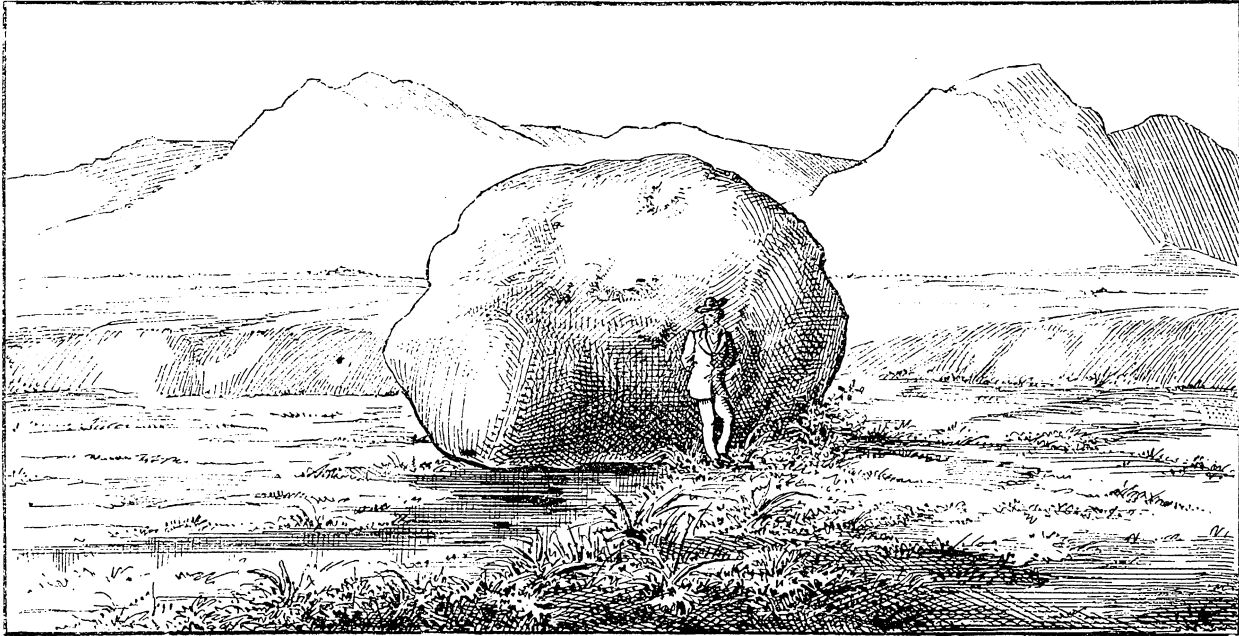
Literature Cited

- Balke, T., P. M. J. Herman, and T. J. Bouma. 2014. Critical transitions in disturbance-driven ecosystems: identifying windows of opportunity for recovery. *Journal of Ecology* 102:700–708.

- Beisner, B., D. Haydon, and K. Cuddington. 2003. Alternative stable states in ecology. *Frontiers in Ecology and the Environment* 1:376–382.
- Biggs, R., S. R. Carpenter, and W. A. Brock. 2009. Turning back from the brink: detecting an impending regime shift in time to avert it. *Proceedings of the National Academy of Sciences of the USA* 106:826–831.
- Brolsma, R. J., D. Karssenberg, and M. F. P. Bierkens. 2010. Vegetation competition model for water and light limitation. I. Model description, one-dimensional competition and the influence of groundwater. *Ecological Modelling* 221:1348–1363.
- Castelletti, A., S. Galelli, M. Ratto, R. Soncini-Sessa, and P. C. Young. 2012. A general framework for dynamic emulation modelling in environmental problems. *Environmental Modelling and Software* 34:5–18.
- Claussen, M., S. Bathiany, V. Brovkin, and T. Kleinen. 2013. Simulated climate-vegetation interaction in semi-arid regions affected by plant diversity. *Nature Geoscience* 6:954–958.
- Davies, A. L., S. Colombo, and N. Hanley. 2014. Improving the application of long-term ecology in conservation and land management. *Journal of Applied Ecology* 51:63–70.
- de Jong, R., S. de Bruin, M. Schaepman, and D. Dent. 2011. Quantitative mapping of global land degradation using earth observations. *International Journal of Remote Sensing* 32:6823–6853.
- Dusar, B., G. Verstraeten, B. Notebaert, and J. Bakker. 2011. Holocene environmental change and its impact on sediment dynamics in the eastern Mediterranean. *Earth-Science Reviews* 108:137–157.
- Heimsath, A. M., and B. C. Burke. 2013. The impact of local geochemical variability on quantifying hillslope soil production and chemical weathering. *Geomorphology* 200:75–88.
- Hughes, T. P., C. Linares, V. Dakos, I. A. van de Leemput, and E. H. van Nes. 2013. Living dangerously on borrowed time during slow, unrecognized regime shifts. *Trends in Ecology and Evolution* 28:149–155.
- Janssen, R. H. H., M. B. J. Meinders, E. H. van Nes, and M. Scheffer. 2008. Microscale vegetation-soil feedback boosts hysteresis in a regional vegetation-climate system. *Global Change Biology* 14:1104–1112.
- Karssenberg, D. 2006. Upscaling of saturated conductivity for Hortonian runoff modelling. *Advances in Water Resources* 29:735–759.
- Kröpelin, S., D. Verschuren, A.-M. Lézine, H. Eggermont, C. Cocquyt, P. Francus, J.-P. Cazet, et al. 2008. Climate-driven ecosystem succession in the Sahara: the past 6000 years. *Science* 320:765–768.
- Larsen, I. J., P. C. Almond, A. Eger, J. O. Stone, D. R. Montgomery, and B. Malcolm. 2014. Rapid soil production and weathering in the Southern Alps, New Zealand. *Science* 343:637–640.
- Ludwig, D., D. D. Jones, and C. S. Holling. 1978. Qualitative analysis of insect outbreak systems: the spruce budworm and forest. *Journal of Animal Ecology* 47:315–332.
- Marrow, P., U. Dieckmann, and R. Law. 1996. Evolutionary dynamics of predator-prey systems: an ecological perspective. *Journal of Mathematical Biology* 34:574–578.
- May, R. M. 1977. Thresholds and breakpoints in ecosystems with a multiplicity of stable states. *Nature* 269:471–477.
- Morgan, R. P. C., and J. H. Duzant. 2008. Modified MMF (Morgan-Morgan-Finney) model for evaluating effects of crops and vegetation cover on soil erosion. *Earth Surface Processes and Landforms* 33:90–106.
- Noy-Meir, I. 1975. Stability of grazing systems: an application of predator-prey graphs. *Journal of Ecology* 63:459–481.
- Oreskes, N., K. Schraderfrechette, and K. Belitz. 1994. Verification, validation, and confirmation of numerical models in the earth sciences. *Science* 263:641–646.
- Pelletier, J. D., G. A. Barron-Gafford, D. D. Breshears, P. D. Brooks, J. Chorover, M. Durcik, C. J. Harman, et al. 2013. Coevolution of nonlinear trends in vegetation, soils, and topography with elevation and slope aspect: a case study in the sky islands of southern Arizona. *Journal of Geophysical Research F: Earth Surface* 118:741–758.
- Pickup, G. 1999. Desertification and climate change—the Australian perspective. *Climate Research* 11:51–63.
- Rietkerk, M., and J. Van De Koppel. 1997. Alternate stable states and threshold effects in semi-arid grazing systems. *Oikos* 79:69–76.
- Rietkerk, M., F. Van Den Bosch, and J. Van De Koppel. 1997. Site-specific properties and irreversible vegetation changes in semi-arid grazing systems. *Oikos* 80:241–252.
- Rinaldi, S., and M. Scheffer. 2000. Geometric analysis of ecological models with slow and fast processes. *Ecosystems* 3:507–521.
- Rodríguez-Iturbe, L., and A. Porporato. 2004. *Ecohydrology of water-controlled ecosystems*. Cambridge University Press, Cambridge.
- Schaetzl, R. J., and S. Anderson. 2005. *Soils: genesis and geomorphology*. Cambridge University Press, Cambridge.
- Scheffer, M. 2009. *Critical transitions in nature and society*. Princeton University Press, Princeton, NJ.
- Scheffer, M., M. Holmgren, V. Brovkin, and M. Claussen. 2005. Synergy between small- and large-scale feedbacks of vegetation on the water cycle. *Global Change Biology* 11:1003–1012.
- Siteur, K., J. Mao, K. G. J. Nierop, M. Rietkerk, S. C. Dekker, and M. B. Eppinga. 2016. Soil water repellency: a potential driver of vegetation dynamics in coastal dunes. *Ecosystems* 19:1210–1224.
- Solé, R. V. 2011. *Phase transitions*. Princeton University Press, Princeton, NJ.
- Stenseth, N. C., W. Falck, O. N. Bjørnstad, and C. J. Krebs. 1997. Population regulation in snowshoe hare and Canadian lynx: asymmetric food web configurations between hare and lynx. *Proceedings of the National Academy of Sciences of the USA* 94:5147–5152.
- Stockmann, U., B. Minasny, and A. B. McBratney. 2014. How fast does soil grow? *Geoderma* 216:48–61.
- Thornes, J. B. 1985. The ecology of erosion. *Geography* 70:222–235.
- . 2007. Modelling soil erosion by grazing: recent developments and new approaches. *Geographical Research* 45:13–26.
- . 2013. Stability and instability in the management of desertification. Pages 399–413 in J. Wainwright and M. Mulligan, eds. *Environmental modelling: finding simplicity in complexity*. Wiley, Chichester.
- Valentin, C., J. Poesen, and Y. Li. 2005. Gully erosion: impacts, factors and control. *Catena* 63:132–153.
- Van Geest, G. J., H. Coops, M. Scheffer, and E. H. Van Nes. 2007. Long transients near the ghost of a stable state in eutrophic shallow lakes with fluctuating water levels. *Ecosystems* 10:36–46.
- Van Nes, E. H., and M. Scheffer. 2005. A strategy to improve the contribution of complex simulation models to ecological theory. *Ecological Modelling* 185:153–164.
- Vicente-Serrano, S. M., A. Zouber, T. Lasanta, and Y. Pueyo. 2012. Dryness is accelerating degradation of vulnerable shrublands in semiarid Mediterranean environments. *Ecological Monographs* 82:407–428.

- Wainwright, J., and A. J. Parsons. 2010. Thornes, J.B. 1985: the ecology of erosion. *Geography* 70, 222–35. *Progress in Physical Geography* 34:399–408.
- Werner, B. T. 1999. Complexity in natural landform patterns. *Science* 284:102–104.
- Willis, K. J., R. M. Bailey, S. A. Bhagwat, and H. J. B. Birks. 2010. Biodiversity baselines, thresholds and resilience: testing predictions and assumptions using palaeoecological data. *Trends in Ecology and Evolution* 25:583–591.
- Yu, W. J., J. Y. Jiao, Y. Chen, D. L. Wang, N. Wang, and H. K. Zhao. 2016. Seed removal due to overland flow on abandoned slopes in the Chinese hilly gullied loess plateau region. *Land Degradation and Development* 28:274–282.
- References Cited Only in the Online Appendixes**
- Ahnert, F. 1987. Process-response models of denudation at different spatial scales. *Catena* 10:31–50.
- Allen, R. G., L. S. Pereira, D. Raes, and M. Smith. 2006. FAO irrigation and drainage paper no. 56. Crop evapotranspiration. Food and Agriculture Organization, Rome.
- Anderson, R. S., and S. P. Anderson. 2010. *Geomorphology*. Cambridge University Press, Cambridge.
- Bergström, S. 1995. The HBV model. Pages 443–476 in V. P. Singh, ed. *Computer models of watershed hydrology*. Water Resources, Highlands Ranch, CO.
- Chow, V. T., D. R. Maidment, and L. W. Mays. 1988. *Applied hydrology*. McGraw-Hill, New York.
- de Roo, A. P. J., C. G. Wesseling, and C. J. Ritsema. 1996. LISEM: a single-event physically based hydrological and soil erosion model for drainage basins. I. Theory, input and output. *Hydrological Processes* 10:1107–1117.
- de Roo, A. P. J., C. G. Wesseling, and W. P. A. Van Deursen. 2000. Physically based river basin modelling within a GIS: the LISFLOOD model. *Hydrological Processes* 14:1981–1992.
- Descheemaeker, K., D. Raes, R. Allen, J. Nyssen, J. Poesen, B. Muys, M. Haile, et al. 2011. Two rapid appraisals of FAO-56 crop coefficients for semiarid natural vegetation of the northern Ethiopian highlands. *Journal of Arid Environments* 75:353–359.
- Edelstein-Keshet, L. 2005. *Mathematical models in biology*. SIAM, Philadelphia.
- Eldridge, D. J., L. Wang, and M. Ruiz-Colmenero. 2015. Shrub encroachment alters the spatial patterns of infiltration. *Ecohydrology* 8:83–93.
- Gómez, J. A., J. V. Giráldez, and E. Fereres. 2001. Rainfall interception by olive trees in relation to leaf area. *Agricultural Water Management* 49:65–76.
- Govers, G. 1990. Empirical relationships for the transport capacity of overland flow. Pages 45–63 in D. E. Walling, A. Yair, and S. Berkowicz, eds. *Erosion, transport and deposition processes*. Proceedings of the Jerusalem Workshop, March–April 1987. International Association of Hydrological Sciences no. 189, Wallingford.
- Hale, M. G., and D. M. Orcutt. 1987. *The physiology of plants under stress*. Wiley, New York.
- Hendriks, M. 2010. *Introduction to physical hydrology*. Oxford University Press, Oxford.
- Hessel, R., and V. Jetten. 2007. Suitability of transport equations in modelling soil erosion for a small Loess Plateau catchment. *Engineering Geology* 91:56–71.
- Hudek, C., G. Sterk, R. L. P. H. van Beek, and S. M. de Jong. 2014. Modelling soil erosion reduction by *Mahonia aquifolium* on hillslopes in Hungary: the impact of soil stabilization by roots. *Catena* 122:159–169.
- Husak, G. J., J. Michaelsen, and C. Funk. 2007. Use of the gamma distribution to represent monthly rainfall in Africa for drought monitoring applications. *International Journal of Climatology* 27:935–944.
- Jiménez-Hornero, F. J., A. Laguna, and J. V. Giráldez. 2005. Evaluation of linear and nonlinear sediment transport equations using hillslope morphology. *Catena* 64:272–280.
- Karssenberg, D., O. Schmitz, P. Salamon, K. De Jong, and M. F. P. Bierkens. 2010. A software framework for construction of process-based stochastic spatio-temporal models and data assimilation. *Environmental Modelling and Software* 25:489–502.
- Katerji, N., M. Mastroianni, and G. Rana. 2008. Water use efficiency of crops cultivated in the Mediterranean region: review and analysis. *European Journal of Agronomy* 28:493–507.
- Kato, T., and M. Kamichika. 2006. Determination of a crop coefficient for evapotranspiration in a sparse sorghum field. *Irrigation and Drainage* 55:165–175.
- Lana-Renault, N., and D. Karssenberg. 2013. PyCatch: component based hydrological catchment modelling. *Cuadernos de Investigación Geográfica* 39:315–333.
- Lilhare, R., V. Garg, and B. R. Nikam. 2015. Application of GIS-coupled modified MMF model to estimate sediment yield on a watershed scale. *Journal of Hydrologic Engineering* 20.
- Ludwig, J. A., B. P. Wilcox, D. D. Breshears, D. J. Tongway, and A. C. Imeson. 2005. Vegetation patches and runoff-erosion as interacting ecohydrological processes in semiarid landscapes. *Ecology* 86:288–297.
- Martin, Y. 2000. Modelling hillslope evolution: linear and nonlinear transport relations. *Geomorphology* 34:1–21.
- McCord, J. T., and D. B. Stephens. 1987. Lateral moisture flow beneath a sandy hillslope without an apparent impeding layer. *Hydrological Processes* 1:225–238.
- Meyer, P. D., M. L. Rockhold, and G. W. Gee. 1997. Uncertainty analyses of infiltration and subsurface flow and transport for SDMP Sites (NUREG/CR-6565, PNNL-11705). US Nuclear Regulatory Commission, Washington, DC.
- Monsi, M., and T. Saeki. 1953. Über den Lichtfaktor in den Pflanzengesellschaften und seine Bedeutung für die Stoffproduktion. *Japanese Journal of Botany* 14:22–52.
- NumPy. 2016. Package for scientific computing with Python. <http://www.numpy.org>.
- PCRaster. 2017. PCRaster: software for environmental modelling. <http://www.pcraster.eu>.
- Rietkerk, M., M. C. Boerlijst, F. Van Langevelde, R. HilleRisLambers, J. Van de Koppel, L. Kumar, H. H. T. Prins, et al. 2002. Self-organization of vegetation in arid ecosystems. *American Naturalist* 160:524–530.
- Schulze, E. D. 1986. Carbon dioxide and water vapor exchange in response to drought in the atmosphere and in the soil. *Annual Review of Plant Physiology* 37:247–274.
- SciPy. 2016. Python-based ecosystem of open-source software for mathematics, science, and engineering. <http://www.scipy.org>.
- SymPy. 2016. Python library for symbolic mathematics. <http://www.sympy.org>.
- Wada, Y., I. E. M. de Graaf, and L. P. H. van Beek. 2016. High-resolution modeling of human and climate impacts on global wa-

- ter resources. *Journal of Advances in Modeling Earth Systems* 8:735–763.
- Williams, L. E., and J. E. Ayars. 2005. Grapevine water use and the crop coefficient are linear functions of the shaded area measured beneath the canopy. *Agricultural and Forest Meteorology* 132: 201–211.
- Woodward, F. I., T. M. Smith, and W. R. Emanuel. 1995. A global land primary productivity and phytogeography model. *Global Biogeochemical Cycles* 9:471–490.
- Associate Editor: Mark Vellend
Editor: Alice A. Winn



“To those who have experienced the pangs of thirst, while journeying over the desolate wastes that characterize this section, it will not be surprising that reminiscences of water should linger longest in the memory of the traveler. . . . A few miles west of Red Mountain Spring, in a dry ravine, through which the traveler passes to reach Fish Lake Valley, is found Mamie Spring [figured]. The water is excellent and plentiful. Its situation is rather unique. In the bottom of a dry wash lies a very large boulder of conglomerate, or more strictly of breccia, transported from some distance, from the under side of which the water of the spring gushes into a little pool or basin it has made for itself. From this basin the water, overflowing, traverses for a few yards the gravelly bed of the wash, when it sinks and is seen no more.” From “The Springs of Southern Nevada” by D. A. Lyle (*The American Naturalist*, 1878, 12:18–27).